Proceedings of the 2002 IEEE/RSJ
Intl. Conference on Intelligent Robots and Systems
EPFL, Lausanne, Switzerland • October 2002

Sensor Management for Local Obstacle Detection in Mobile Robots

Juan C. Alvarez[1], Rafael C. González[1], Diego A. Prieto[1], Andrei Shkel[2], V. Lumelsky[3]

[1]*Dept. of Electrical & Computer Eng., University of Oviedo, Gijón, España, juan@ieee.org*
[2]*Dept. of Electrical & Computer Eng., University of California, Irvine, USA, ashkel@uci.edu*
[3]*Dept. of Mechanical Engineering, University of Wisconsin, Madison, USA, lumelsky@engr.wisc.edu*

Abstract

In experimental robotics it is common to complement the motion planning algorithm with a local obstacle avoidance module. We are concerned here with the specifications of a range sensor specifically design for the task. Such sensor has special requirements: it has to guarantee detection and response, and it has to guarantee throughput, providing information at a rate in proportion to robot velocity. An analysis is presented which allows the selection of the sensor requirements for collision avoidance tasks in mobile robots. The design takes into account robot dynamics, it is compatible with fast motion –only the indispensable environment zones are explored– and avoids unnecessary velocity reductions. Experiments show the possibilities and limitations of the approach.

1 Introduction

This paper is concerned with the design of a range sensor used for collision–avoidance tasks in mobile robots. Being robot motion planning a difficult problem, some simplifying assumptions are usually made, such as stationary environment, no actuator dynamics, flat terrain or perfect sensor information. Since in real robots these assumptions are easily violated, it is common to complement the motion planning algorithm with a "local obstacle avoidance" module. It is a sensor-based task, whose aim is to let the robot reach intermediate goals –as provided by the global planner– while avoiding "unexpected" (from the planner point of view) obstacles.

The task nature imposes two key requirements on the sensor: it has to guarantee throughput, providing information at a time rate fast enough to deal with the robot velocity and dynamics. And it has to guarantee detection, by providing information enough to let the robot react adequately to any potential danger. Notice the difficulty for detection guarantee in Figure 1-left: a sensor oriented toward the direction of motion does not sweep some possible motion trajectories, a tunnel–vision problem [1].

Throughput and detection guarantee are opposite demands. If we try to assure the latter by augmenting the scanned area in the robot's surroundings, it will increase the time taken to process the sensor data, decreasing proportionally the reactivity to the external world. This trade-off can be addresed by a "moving while processing" strategy, but it will adversaly affect the motion planner performance [2]·

Our approach is based on finding the minimum information needed to guarantee the safety of motion. Problem formulation and limits are discussed in Section 2. Section 3 is devoted to the analysis of the sensor requirements; robot dynamics and motion control policy are included in the design. The solution includes a sensor management strategy to pan the sensor in order to eliminate the tunnel effect, see Section 4. The resulting specifications can be implemented with various sensor technologies, such as ultrasonics or CCD cameras. Experimental results (Section 5) show the feasibility of the proposed strategy, allowing a mobile robot to move at high average speeds.

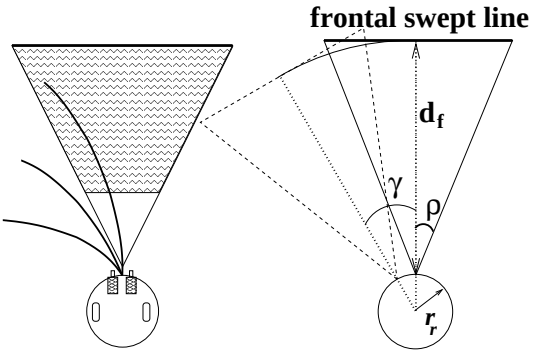

Figure 1: *Design of a "collision–detection" sensor: Left: Tunnel vision problem. Right: Sensor Field of Regard: it is defined by the Field of View ρ, the Depth of Field d_f, and the pan angle direction γ.*

2 Problem Definition

We address the problem of a robot $\mathcal{A}$ moving in a planar 2D Euclidean environment $\mathcal{W}$=$\mathbb{R}^2$ of associated Cartesian frame $\mathcal{F}_\mathcal{W}$. $\mathcal{A}$ has a circular shape with radius r_r, and its configuration is represented by $\mathbf{q}(t) = (x, y, \theta)$,

the coordinates of its center $\mathbf{C_i} = (x, y)$ and its orientation θ relative to the coordinate system $\mathcal{F}_\mathcal{W}$. Orientation θ, a mobile frame $\mathcal{F}_\mathcal{A}$ attached to the robot center, and the instantaneous velocity vector, are collinear.

The robot is equipped with range sensors, which can sweep an area in front of the robot called *field of regard*, see Figure 1-right. It is defined by the aperture angle (*field of view*, ρ), and its maximum range (*depth of field*, d_f). The sensor is able to pan, represented by a rotation angle γ relative to the mobile frame $\mathcal{F}_\mathcal{A}$. The "frontal swept line" (FSL) is chosen to be perpendicular and symmetrical with respect to the mobile frame, and it is defined by parameters (d_f, ρ, γ). This paper is about the task-dependent selection of these three parameters.

Robot motion decisions are computed in short and fixed time periods T_{cyc}. At every period T_{cyc} a new intermediate goal to reach $\mathbf{T_i}$ is provided to the robot (we can think of $\mathbf{T_i}$ as the result of a motion planning module). The robot has a motion control strategy, designed to approach $\mathbf{T_i}$ with some optimal criteria (such as minimum time).

The operation mode of the sensor will be as follows: the whole triangular area defined by the FSL is scanned within one cycle, and the distance to the closer object inside this area is returned. For design purposes, we will consider that the "correct" sensor operation occurs whenever the obstacles are first swept by the FSL. Then, the distance measured to any obstacle in its first appearance should be d_f.

The problem at hand is to calculate the sensor field of regard dimensions and panning strategy in order to guarantee robot safety. Safety means 1) the robot is able to avoid any obstacle that appears within its field of regard, and 2) its sensors completely sweep the whole area traversed by the robot during its motion.

Two robot characteristics will affect the design: its mobility limitations and its motion control strategy. Mobility limitations come from the robot mechanical configuration, dynamics, and other physical limits. Usual steering mechanisms impose a nonholonomic restriction,

$$\dot{x} = v\cos\theta \qquad \dot{y} = v\sin\theta \qquad \dot{\theta} = \omega \tag{1}$$

where robot position depends on its forward velocity $v(t)$, and its rate of change in orientation or turn velocity $\omega(t)$. Robot actuator dynamics limit robot velocities (v, ω) both in magnitude $[v_M, \omega_M]$ and in rate of change or acceleration, $[a_M, \alpha_M]$. A convenient model for robots with asynchronous steering mechanism is [3]:

$$\dot{v} + k_p v = u_v \qquad \dot{\omega} + k_h \omega = u_\omega \tag{2}$$

being k_p and k_h constants and (u_v, u_ω) velocity references to the robot actuators. The robot trajectory for a given control command (u_v, u_ω) can be computed by integrating equations (2) and (1).

The motion control strategy is how the references (u_v, u_ω) are selected from an initial robot position $\mathbf{C_i}$ and state (v_0, ω_0), in order to reach an intermediate goal $\mathbf{T_i}$ with a certain criteria (e.g. in minimum time). For instance, a reasonable strategy for an "emergency stop" is $(u_v, u_\omega) = (0, 0)$. For the rest of operations we will assume that controls are obtained with a maximum turn strategy [4]:

$$u_v = K_v d_{obs} \qquad u_\omega = K_\omega(\mathbf{T}_i - \mathbf{C}_i) \tag{3}$$

with constants K_v and K_ω tuned to maximize velocities, and d_{obs} the sensed distance to the closer obstacle in the intended robot trajectory.

3 Field of Regard Dimensions

The Field of Regard dimensions are limited by basic safety considerations that arise from the robot motion restrictions and control strategy. Let us consider the safety of motion at constant velocities, that is, straight and circular motion.

3.1 Straight Line Motion Considerations

When the robot moves along a straight line, the relation between sensor depth and aperture (d_f, ρ) has to be enough to guarantee its safety. That is accomplished if the whole area traversed by the robot is previously swept by the FSL. It means that, for a circular robot of radius r_r and a sensor of aperture ρ, the field of regard depth satisfies:

$$d_f^a = \frac{r_r}{\tan\rho} \tag{4}$$

If d_f is smaller than d_f^a, safety is not guaranteed. If it is bigger, obstacles out of the robot path will be detected as dangerous, and control (3) will cause an unnecessary reduction of velocity.

A second condition is that sensor field depth d_f has to be large enough to let the robot stop safely –fast enough– if an obstacle is detected in front of it. This distance will be larger as the robot inertia is bigger. Let us call an "emergency stop" the maneuver aimed to completely stop the robot, whatever its initial state $(v, \omega) = (v_0, \omega_0)$ is. Such maneuver will be implemented by sending the command references $(u_v, u_\omega) = (0, 0)$,

The distance traversed before the control command halts the robot, r_d, depends on its dynamics and the response time of the robot control system, t_r,

$$r_d = v_0 t_r + x(\infty) = v_0 t_r + \frac{v_0}{k_p} \tag{5}$$

being $x(\infty) = \frac{v_0}{k_p}$ the consequence of dynamics, calculated by integrating equations (2) and (1) [3]. This magnitude establish a lower limit to the depth of field, $d_f \geq r_d$, which depends on the robot current status v_0. The worst

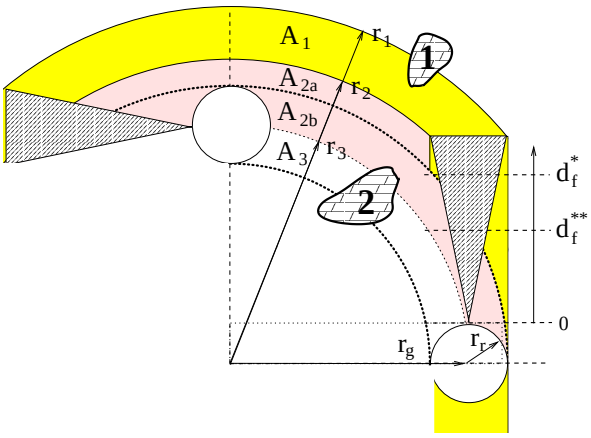

Figure 2: *Robot with a sensor Field of Regard fulfilling conditions* (4) *and* (6)*, when turning with constant velocity: the tunnel vision problem.*

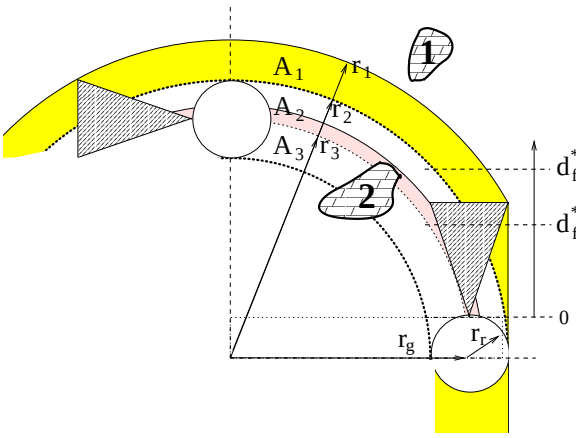

Figure 3: *A sensor with field fulfilling* (4) *and* (6) *and* $d_f^{**} > d_f > d_f^*$.

case analysis $v_0 = v_{\max}$ let us to compute, off–line, a secure distance to stop, for every initial state $(v_0, \omega = 0)_k$:

$$d_f^b \geq r_{d_{\max}} \tag{6}$$

As conclusion, when moving in a straight line, robot safety and smooth motion is guaranteed by equations (4) and (6).

3.2 Constant Velocity Turning Considerations

The model defined by (1) and (2) shows that, for constant velocity references (u_v, u_ω), the robot moves along a circular trajectory of radius $r_g = u_v/u_\omega$. Then, for a sensor field of view fulfilling conditions (4) and (6), we can identify potential risky situations, see Figure 2.

The FSL sweeps the area A_1, which extends between circular sectors of radius r_2 and r_1. The obstacles inside A_1 will produce a lineal robot velocity because of the control law (3). But, as zone A_1 was not going to be traversed by the robot, it is a situation of "unnecessary deceleration".

The area comprised between sectors of radius r_3 and r_2 (A_2) is a zone of "lateral detection": an obstacle inside will appear abruptly on the robot field of view. It makes the lineal velocity-reduction strategy not useful to avoid collisions, probably triggering some kind of "immediate collision" alarm. Notice that it might happen even if the A_2 obstacle is not interfering with the intended robot trajectory, zone A_{2a}.

Finally, A_3 is a "blind zone", where obstacles are not detected (the mentioned tunnel problem).

These considerations suggest new conditions on the selection of the sensor field depth d_f. The objective is to sweep in advance with the FSL exactly the zone that will be traversed by the robot, as we did in straight line motion. In other words, we want to eliminate A_1, A_2, and A_3 areas. Notice in Figure 2 that smaller depths d_f reduce them, in opposition to the demand of larger depths–at least fulfilling condition (6)–that increases the options to react to unexpected obstacles. This trade-off depends on two factors:

1) There is a certain limit depth, d_f^*, that eliminates lateral detection of non dangerous obstacles (zone A_{2a}). As $d_f \leq d_f^*$, more robot size is swept by the FSL. Larger $d_f \geq d_f^*$ are only justified in order to implement more complex re-planning strategies to avoid the unexpected obstacle. This value d_f^* is an upper limit to d_f, and can be obtained from (see Appendix):

$$d_f{}^* = 2\sqrt{r_r r_g} - r_r \tag{7}$$

2) Another limit value exists d_f^{**}; smaller depths $d_f \leq d_f^{**}$ completely eliminates lateral detection (zone A_2):

$$d_f^{**} = \sqrt{2}\sqrt{r_r r_g} - r_r \tag{8}$$

A further reduction of blind zones A_3 is only possible by choosing $d_f < d_f^{**}$.

For a given d_f, we can quantify the "risk" of the events "unnecessary deceleration", "lateral detection" , and "blind zone", as the relation of areas A_i to the total terrain extension covered by the robot, $r_{A_i} = A_i/4\pi r_r r_g$. Defining $p = (d_f + r_r)^2/4r_r r_g$, three situations might occur depending on d_f (see Figure 3):

1) if $d_f > d_f^*$: $r_{A_1} = 1, r_{A_2} = p - 0.5, r_{A_3} = 0.5$
As $d_f \to d_f^*$, the risk factor r_{A_2} tends to one, and the risk of a lateral detection of a harmless obstacle (area A_{2a}) vanishes. There are no active detection with the FSL.

2) if $d_f^{**} > d_f > d_f^*$: $r_{A_1} = p, r_{A_2} = 0.5, r_{A_3} = 0.5$
Unnecessary detection risk is diminished, because part of the FSL is starting to be employed in "useful" detection.

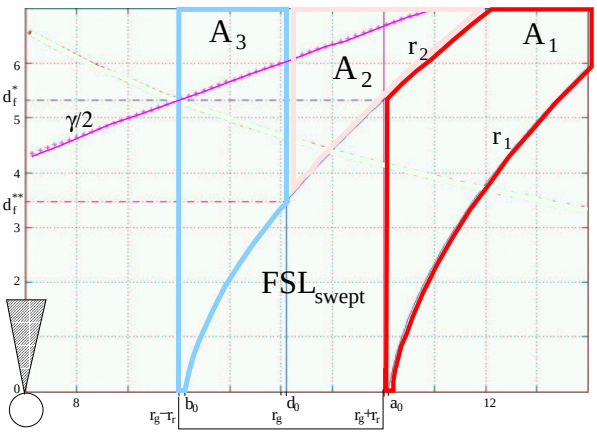

Figure 4: *Sensor generated conditions (A_1, A_2, and A_3 zones) as a function of the depth of field d_f ($r_g = 10r_r$). Solution to equation* (9)*, giving the "safer sensor" panning γ as a function of the depth of field d_f, is plotted.*

A_2 zone remains constant because lateral detection risk reduces ($r_{A_{2b}} \rightarrow 0$) at the same rate that FSL detection grows.

3) if $d_f^{**} > d_f > 0$: $r_{A_1} = r_{A_3} = p, r_{A_{2b}} = 0$
Blind area and useless detection areas are equal and constant, while lateral detection danger disappears. Notice that even for a robot without dynamics (able to stop on site and allowing us to choose $d_f = 0$), the blind zone A_3 does not completely disappear.

Figure 4 represents the previous analysis for a turn radius of $r_g = 10r_r$. Lines r_1, r_2 and robot dimensions $r_g \pm r_r$ are plotted as a function of depth d_f (condition (4) fixes the sensor aperture ρ). For a given depth (vertical axe), we can see what part of the robot size (represented between vertical lines $r_g - r_r$ and $r_g + r_r$) will move over each A_i zone.

4 Sensor Panning Strategy

It is clear that the previous static design is not enough to eliminate the risk of crossing areas of lateral detection or blind zones. An alternative to reduce such dangers is to dynamically accommodate the scanned area to the instantaneous robot motion state. Let us define the scanning swept line by the pair (d_f, ρ), and let us denote γ to the angle, measured from the main robot axis, to direct a new scan action.

In theory, we have three variables to select in order to cover the robot motion area: (γ, d_f, ρ). Previous analysis recommended to fix $\tan \rho = \frac{r_r}{d_f}$, leaving (γ, d_f) as possible elections. We will calculate γ assuming that the scan line has the previous calculated shape d_f, and adding the panning capability.

The proposed solution consists of finding the sensor orientation γ such as the blind zone A_3 diminishes the most, or totally disappears. The idea is to make use of the whole FSL to cover the intended robot trajectory. Let us call it the "safer sensor" strategy.

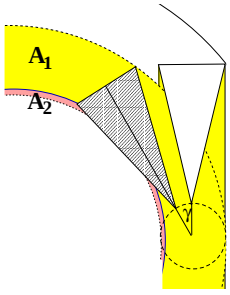

Figure 5: *The "safer sensor" panning strategy: the sensor orientation γ is selected in order to eliminate blind zones A_3*

Making the superior side of the FSL equal to the external radio $r_g + r_r$ of the robot trajectory, see Figure 5, γ can be obtained from solving the equation (see Appendix):

$$A \sin \gamma + B \cos \gamma = 1 \qquad (9)$$

being A and B constants for a given field of regard (d_f, ρ). Its solution reveals the bigger blind-zone reduction that can be achieved by panning.

In Figure 4 the solution of (9) is plotted. For a given depth d_f, the horizontal axe represents $\gamma/2$ (in degrees). For example, a window of depth $d_f = 5$ requieres a panning of $\gamma = 17$ degrees (per r_r unit). Notice that A_2 zones still may appear. To avoid them, an alternative design would be necessary which allows us to modify the three sensor parameters on-line, a condition much more complicated to apply in real sensors.

5 Experiments

The sensor model presented is general enough to be implemented with various different sensing devices. But in practice, some restrictions in the election of the parameters will be applied, depending on the specific system characteristics. For example, in a rotating sonar sensor, angle ρ could be the beam semi-aperture, d_f the effective maximum range, and γ the pan angle. With a sonar ring, transducers are arranged around the robot with fixed intervals γ_k, and only those pan angles are allowed. By using computer vision for range measurement we may have more flexibility, but restrictions will exist over the other two parameters [5].

The previous analysis was applied to the design of the obstacle avoidance module of two mobile robots, a Nomad–200 and a B-21. They both have a diameter of 53 cm and synchronous steering mechanism, allowing to command

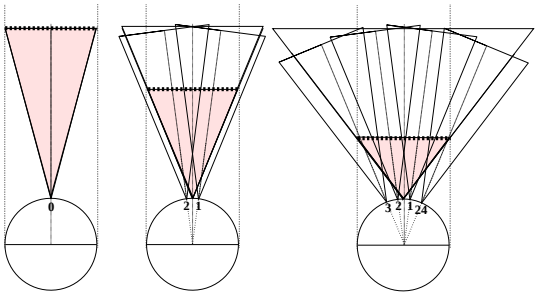

Figure 6: *(Left) Sensor implemented with a frontal ultrasonic sensor, robot Nomad-200, aperture 15 deg. (Center) Sensor implemented with two sonar sensors, located at ± 7.5 degrees from the main robot axis, robot B-21, aperture 22.5 deg. (Right) Sensor implemented with four sonar sensors, located at ± 7.5 degrees from the main robot axis, robot B-21, aperture 37.5 deg.*

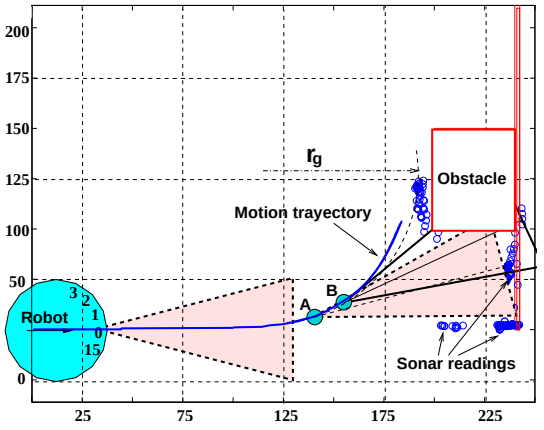

Figure 7: *Stop maneuver triggered by an "A_2 zone" obstacle; top view. From point A to point B the robot is turning at maximum speed, and the sensor is measuring a maximum distance d_f; in B the obstacle corner comes into view, and an abrupt range measure is read, leading to an emergency stop condition (and eventually a collision).*

forward and turning velocities separately. The strategy was implemented with ultrasonic range sensors. They are equipped with sonar rings of equidistant 16 and 24 units respectively. It limits our pan angle election to angles multiple of 22.4 and 15 degrees respectively. Notice how different combinations of sonar firing can be used to implement a needed scan window, Figure 6.

In the first experiment the robot was commanded at maximum velocities of $(v_M, \omega_M) = (60cm/s, 45°/s)$ and maximum accelerations of $(a_M, \alpha_M) = (25cm/s^2, 50°/s^2)$. It means a maximum radius of turn of r_g=v/w=78 cm.

First, we test the implementation with a frontal sonar sensor, see Figure 6-left [6]. The Polaroid sonar has a beam semi-width of around 15 degrees, and condition (4) fixes d_f=99 cm. Experiments with the robot dynamic response show that this is the same distance needed to stop the robot moving at its highest speed 61 cm/s [3].

Limiting values, given by equations (7) and (8) are 59.5 cm and 34.3 cm respectively. It means that the selected depth of d_f =99 centimeters will present blind and lateral detection zones. The best sensor is given by equation (9), at 54.17 degrees, between the second (45 deg) and the third (67.5 deg).

Figure 7 shows how, with no sensor panning, an obstacle in a A_2 zone ("lateral detection") appears abruptly on the robot field of view and triggers an emergency stop condition.

Similar things happen to the second robot when moving at its maximum forward velocity, 1 m/s. With a 45 degrees beam, see Figure 6-center, the d_f to cover condition (4) is 64 cm. As this distance is similar to the needed to stop, $d_f \approx d_f^*$, the limiting values (7) and (8) are again 59.5 cm and 34.3 cm respectively, as r_r and r_g do not change. It means that, with the selected height of d_f =64 centimeters, the sensor will not present lateral detection zones.

The proposed sensor panning strategy, equation (9), suggests to fire the sonar located at 32.5 degrees, that can be physically accomplished with sonars 3 and 4 (see Figure 6-center) (30 degrees position). It eliminates blind zones, and the obstacle is detected with time enough to reduce speed and eventually, plan a detour.

6 Conclusions

An analysis is presented which allows the selection of the sensor requirements for collision avoidance tasks of mobile robots. The design takes into account robot dynamics, given by a mathematical model. It is compatible with motion in real time, as only the indispensable environment zones are explored, avoiding unnecessary velocity reductions. Perception system restrictions can be considered in the strategy. The analysis is deterministic, and the effect of sensor uncertainties is not discussed.

Appendix: Geometry of turning and panning

Figure 8 shows the geometry of a circular motion. The external radius are:

$$\begin{aligned} r_1^2 &= (r_g + d_f \tan\delta)^2 + (d_f + r_r)^2 \\ r_2^2 &= (r_g - d_f \tan\delta)^2 + (d_f + r_r)^2 \\ r_3^2 &= r_g^2 + r_r^2 \end{aligned}$$

and doing $d_f \tan\delta = r_r$ leads to:

$$\begin{aligned} r_1^2 &= (r_g + r_r)^2 + (d_f + r_r)^2 \\ r_2^2 &= (r_g - r_r)^2 + (d_f + r_r)^2 \\ r_3^2 &= (r_g - r_r)^2 + 2r_r r_g \end{aligned}$$

For given r_r and r_g it can be rewritten as:

$$\begin{aligned} r_1^2 &= a_0 + 2r_r d_f + {d_f}^2 \\ r_2^2 &= b_0 + 2r_r d_f + {d_f}^2 \\ r_3^2 &= d_0 \end{aligned}$$

being (a_0, d_0, c_0) constants dependent on r_r and r_g:

$$\begin{aligned} a_0 &= (r_g + r_r)^2 + {r_r}^2 \\ b_0 &= (r_g - r_r)^2 + {r_r}^2 \\ d_0 &= r_g^2 + r_r^2 \end{aligned}$$

Notice that the following precedence relation applies (for $r_r > 0$):

$$(r_g - r_r)^2 < b_0 < d_0 < (r_g + r_r)^2 < a_0$$

The area swept in a complete 360 degrees turn is:

$$\begin{aligned} A_1 = \pi(r_1^2 - r_2^2) &= 4\pi r_r r_g \\ A_2 = \pi(r_2^2 - r_3^2) &= \pi\left((d_f + r_r)^2 - 2r_r r_g\right) \\ A_3 &= 2\pi r_r r_g \\ A_3^a &= \pi r_r^2 \end{aligned}$$

being $r_3^a = (r_g - r_r)^2 + r_r^2$. The robot swept an area of $\pi(r_g + r_r)^2 - \pi(r_g - r_r)^2 = 4\pi r_g r_r$ in a 360 degrees circular turn.

Notice that A_1 and A_3 do not depend on d_f, and $A_2 + A_3 = \pi(d_f + r_r)^2$.

The limit value d_f^* is such as $A_2^a = 0$, or $r_2 = r_g + r_r$:

$$\begin{aligned} (r_g - r_r)^2 + (d_f + r_r)^2 &= (r_g + r_r)^2 \\ d_f^2 + 2r_r d_f + (r_r^2 - 4r_r r_g) &= 0 \end{aligned}$$

second order equation with solution $d_f^* = \sqrt{4r_r r_g} - r_r$.

The limit value d_f^{**} makes $A_2 = 0$, or $r_2 = r_3 = (r_g - r_r)^2 + 2r_r r_g$, leading to:

$$\begin{aligned} (d_f + r_r)^2 - 2r_g d_f &= 0 \\ d_f^2 + 2r_r d_f + (r_r^2 - 2r_r r_g) &= 0 \end{aligned}$$

again a second order equation with solution $d_f^{**} = \sqrt{2r_r r_g} - r_r$.

The "safer sensor" pan can be derived by making the radius of point P in Figure 8 equal to $r_g + r_r$. It leads to the equation:

$$A_0 \sin\gamma + B_0 \cos\gamma = C_0 \qquad (10)$$

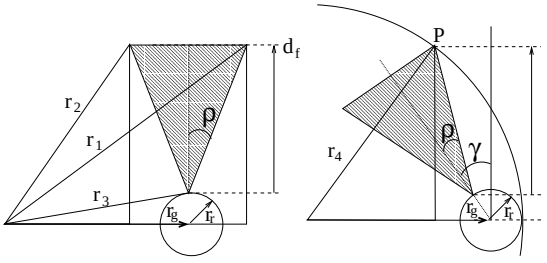

Figure 8: *Geometry of (a) No panning; (b) Pan γ.*

begin $A = A_0/C_0$ and $B = B_0/C_0$ constants for a given field of regard (d_f, ρ):

$$\begin{aligned} A_0 &= r_g + \frac{d_f^2 r_g}{m\cos\rho r_r} \\ B_0 &= -\frac{r_g d_f}{m\cos\rho} \\ C_0 &= \frac{d_f^2}{2r_r\cos^2\rho} - r_g + d_f \end{aligned}$$

The solution to this equation is:

$$\left[\ \arctan\tfrac{A-BU}{B+AU}, \arctan\tfrac{A+BU}{B-AU}\ \right]$$

being:

$$U = \sqrt{B^2 + A^2 - 1}$$

References

[1] Alonzo Kelly and Anthony Stentz, "Analysis of requeriments for high speed rough terrain autonomous mobility. part 1: Throughput and response," in *IEEE Int. Conf. on Robotics and Automation*, Albuquerque, NM, april 1997, pp. 3318–3325.

[2] I. Moon, Jun Miura, and Y. Shirai, "On-line viewpoint and motion planning for efficient visual navigation under uncertainty," *Robotics and Autonomous Systems*, vol. 28, pp. 237–248, 1999.

[3] Juan C. Alvarez, A. Shkel, and V. Lumelsky, "Accounting for mobile robot dynamics in sensor–based motion planning," *Int. Journal of Robotics & Automation*, vol. 16, no. 3, pp. 132–141, 2001.

[4] A. Shkel and V. Lumelsky, "The jogger's problem: Control of dynamics in real-time motion planning," *Automatica*, vol. 33, no. 7, pp. 1219–1233, jul 1997.

[5] R. C. González, J. Cancelas, J. C. Alvarez, J. A. Fernández, and J. M. Enguita, "Fast stereo vision algorithm for robotic applications," in *7th IEEE Int. Conference on Emerging Technologies and Factory Automation, Barcelona, Spain*, 1999, pp. 97–104.

[6] Juan C. Alvarez, A. Shkel, and V. Lumelsky, "Active sensing in sensor-based motion planning with dynamics," in *IMEKO/IFAC/IFIP Workshop on Advanced Robot Systems and Virtual Reality - ISMCR*, 2000.